



# Physicochemical and structural characterization of a polyionic matrix of interest in biotechnology, in the pharmaceutical and biomedical fields

Delphine Magnin<sup>a</sup>, Jacques Lefebvre<sup>b</sup>, Esteban Chornet<sup>a</sup>, Severian Dumitriu<sup>a,\*</sup>

<sup>a</sup>Department of Chemical Engineering, Sherbrooke University, 2500 Boulevard de l'Université, Sherbrooke, Que., Canada J1K 2R1

<sup>b</sup>Unité, de Physico-Chimie des Macromolécules, INRA, Rue de la Géraudière, BP 71627, 44316 Nantes Cedex 3, France

Accepted 15 November 2003

## Abstract

This paper reports on the swelling degree and the rheological and structural characteristics of a hydrogel composed by chitosan and xanthan. The latter is a polyionic hydrogel obtained by complexation between the both polysaccharides. The swelling degree has been found to be influenced by the time of coacervation, the pH of the solution of chitosan used to form the hydrogel and the pH of the swelling solution. The molecular weight and the degree of acetylation of the chitosan also influence the swelling degree of this matrix. The connectivity between chitosan and xanthan affects the swelling degree of this matrix. A rheological study has been carried out in order to understand the formation of the coacervate and of the subsequent hydrogel. The evolution of the storage modulus with time during the coacervation has allowed to optimize the time of coacervation required for a subsequently hydrogel, with desirable swelling degree. The kinetics has shown that (a) the coacervate is formed in two distinct steps and (b) the storage modulus of the hydrogel reaches a stable plateau. The values of the storage modulus have been correlated with the swelling degree. The microscopic characterization has shown the presence of a porous network with a fibrillar structure. To complete the characterization studies fine powder of this hydrogel has been used to determine the surface, perimeter, Feret diameter and sphericity factor distribution of dry and hydrated (swollen) particles.

© 2003 Elsevier Ltd. All rights reserved.

**Keywords:** Polyionic complex; Chitosan; Xanthan; Rheology and structure

## 1. Introduction

This hydrogel is formed by ionic bonding and van der Waals interactions between two biopolymers: chitosan and xanthan (Dumitriu, Chornet, & Vidal, 1995a; Dumitriu, Magny, Montagne, Vidal, & Chornet, 1994).

Chitosan is a linear binary heteropolysaccharide composed of  $\beta$ -(1  $\rightarrow$  4)-2-amino-2-deoxy-D-glucopyranose and of  $\beta$ -(1  $\rightarrow$  4)-2-acetamino-2-deoxy-D-glucopyranose, obtained by alkaline deacetylation of chitin, poly( $\beta$ -(1  $\rightarrow$  4)-2-acetamino-2-deoxy-D-glucopyranose). Chitin, the second most abundant biopolymer after cellulose, is a natural polysaccharide found in the shells of crustaceans such as crabs and shrimps, the cuticle of insects and the cell walls of fungi. Due to their biocompatibility,

biodegradability and other favourable properties, chitin and chitosan have found applications in several sectors: biomedical, pharmaceuticals, food additives, antimicrobial agents, paper and textiles, environmental remediation and other industrial areas (Muzzarelli, 1998; Struszczyk, 2002a–c; Struszczyk, Wawro, & Niekraszewicz, 1989).

Xanthan is an extracellular heteropolysaccharide produced by *Xanthomonas campestris*. It consists of D-glucose, D-mannose, D-glucuronic acid and pyruvate. Xanthan has a cellulosic backbone and a trisaccharide side chain on every second glucose residue:  $\alpha$ -mannose,  $\alpha$ -glucuronic acid and  $\beta$ -mannose compose the trisaccharide side chain. Pyruvic acid diketal groups are located at the 4,6-position of the terminal mannose (Stokke, Christensen, & Smidsrod, 1998). Xanthan is one of the most applied microbial polysaccharides in food (Dhami et al., 1995; Quemener, Marot, Mouillet, Riz, & Diris, 2000; Wang, Wang, & Sun, 2002), pharmaceuticals (Gohel, Amin, Patel, & Panchal, 2002; Kondo, Irie, & Uekama, 1996; Talukdar et al., 1998) and in the biomedical field (Stokke et al., 1998).

\* Corresponding author. Tel.: +1-819-821 7171; fax: +1-819-821 7955.

E-mail addresses: [severian.dumitriu@usherbrooke.ca](mailto:severian.dumitriu@usherbrooke.ca) (S. Dumitriu), [delphine.magnin@usherbrooke.ca](mailto:delphine.magnin@usherbrooke.ca) (D. Magnin), [lefebvre@nantes.inra.fr](mailto:lefebvre@nantes.inra.fr) (J. Lefebvre), [esteban.chornet@usherbrooke.ca](mailto:esteban.chornet@usherbrooke.ca) (E. Chornet).

Many polyionic complexes use chitosan as polycation. Kikuchi and Fukuda (1974) have shown that the chemical structure, the molecular weight, the flexibility, functional groups and hydrophobicity have an effect on the formation of complexes of chitosan–polyanion. Moreover, the conditions of the reaction such as pH, polymer concentration, ionic strength, temperature and the ratio between chitosan and polyanion influence the complexation (Kubota & Kikuchi, 1998; Yamauchi, 2001). Anionic polysaccharides, that have been reported as forming complexes with chitosan are sodium dextran sulfate (Kikuchi & Fukuda, 1974), heparin (Kikuchi & Noda, 1976), carboxymethylcellulose (Fukuda, 1980), carrageenan (Sakiyama, Chu, & Yano, 1993), sodium alginate (Daly & Knorr, 1988), sodium carboxymethyl-dextran (Fukuda & Kikuchi, 1978), chondroitin sulfate (Denuziere, Ferrier, & Domard, 1996) and xanthan (Dumitriu et al., 1994).

Hydrogels are hydrophilic three-dimensional (3D) polymeric networks that can absorb much more water than their own weight so as to provide ideal aqueous conditions for biocompatible applications (Dumitriu & Chornet, 1998a) and for environmentally sensitive bioactive materials such as proteins and specific compounds (Park, Lu, & Crotts, 1995). The formation of a 3D network structure has an important advantage, in that, the gelation increases the mechanical and chemical stability (Dumitriu, Vidal, & Chornet, 1998).

The formation of the polyionic matrix is shown in Fig. 1. The formation of this hydrogel is carried out in many steps. The first one is the mixing of the two solutions of macromolecules. The second step is a modification of concentration of each polymer in the final solution due to the mixing and modification of the structure of the macromolecule. This is due to the change of the local pH (pH 6.8) since the solutions of chitosan and xanthan do not have the same pH. The third step is the formation of polyionic interactions between the  $\text{NH}_3^+$  in chitosan and  $\text{COO}^-$  in xanthan. The steps 2 and 3 correspond to coacervation, which is a well-known described phenomenon. (Tsung & Burgess, 1997). Coacervation is the separation of aqueous polymeric solutions into two immiscible phases: a coacervate phase (concentrated in polymers) and a dilute phase (Tsung & Burgess, 1997). The ionic interaction between chitosan and xanthan has been already proved by infrared spectrum (Dumitriu et al., 1994) and by the evolution of the rheological parameter of the system (Section 3.4). The coacervate obtained is composed of chitosan, xanthan and oriented and non-oriented water molecules. In fact, during the coacervation, the water molecules are entrapped between the macromolecules. The water molecules arrange themselves in layers. The first layer is at the surface of the macromolecules and in this layer the water molecules are oriented via hydrogen bonding. The second layer corresponds to the free (non-oriented) water molecules. This organization of water molecules is the same as that of the organization of water in silica gel (Brinker &

Scherer, 1990). Finally, the last step corresponds to the structural modification of the macromolecular chains by mixing and results in the formation of the hydrogel. In this step, the non-oriented water is eliminated by the mixing strength.

Due to its structure and properties, this hydrogel is particularly attractive as a matrix for enzyme immobilization (Dumitriu & Chornet, 1998b; Dumitriu, Chornet, Vidal, & Moresoli, 1995b; Dumitriu et al., 1994; Magnin, Dumitriu, & Chornet, 2002; Magnin, Dumitriu, Magny, & Chornet, 2001). This matrix is a hydrophilic microenvironment favourable for the inclusion and the stability of the enzymes. In 1994, Dumitriu et al. (1994) demonstrated that the co-immobilization of protease and xylanase led to a synergistic effect (Dumitriu et al., 1994). In a more recent study, Magnin et al. (2002) have shown the influence of the concentration of enzyme, the storage temperature and the molarity of the buffer storage medium, on the catalytic activity. Lipase immobilization into this matrix doubles its enzymatic activity in aqueous media (Magnin et al., 2001). They are also active in organic media (Magnin et al., 2001). Moreover, the immobilization of lipase protects the enzyme against thermal degradation and excellent activity is obtained at 55 °C (Magnin et al., 2001). A distinct application of this matrix is in the pharmaceutical field (Jshizawa, 2002), where it has been used to enhance the dissolution rate of water insoluble drugs, and, consequently, increase their bioavailability. Such approach has been proven with fenofibrate, ursodeoxycholic acid, nifedipine and indomethacin (Jshizawa, 2002; Jshizawa, Dumitriu, & Chornet, 2001). This polyionic hydrogel can also be used in dermocosmetics. Vitamins in this matrix are protected against rapid oxidation (Dumitriu & Chornet, 2000). Recently, the inclusion of an antibiotic polypeptide has been investigated in order to decrease the solubility of this drug (Magnin et al., 2002).

In this paper, we discuss the physicochemical and structural characteristics of this hydrogel. Its swelling properties are studied in relation with the fibrillar network connectivity within the hydrogel. The kinetic study of the coacervation is carried out via rheological measurements and in addition, microscopic characterization is used to characterize the porous structure and the internal microstructure of the matrix.

## 2. Materials and methods

### 2.1. Preparation and characterization of chitosan and xanthan solution

Chitosan samples (CH 79 and CH 71P), from shrimp shells, were provided by Kemestrie, Inc. (Sherbrooke, Que., Canada) and (CH V) by Vanson, Inc. (Redmond, WA, USA). Chitosan was characterized by its molecular weight and degree of acetylation (DA). Chitosan preparation and

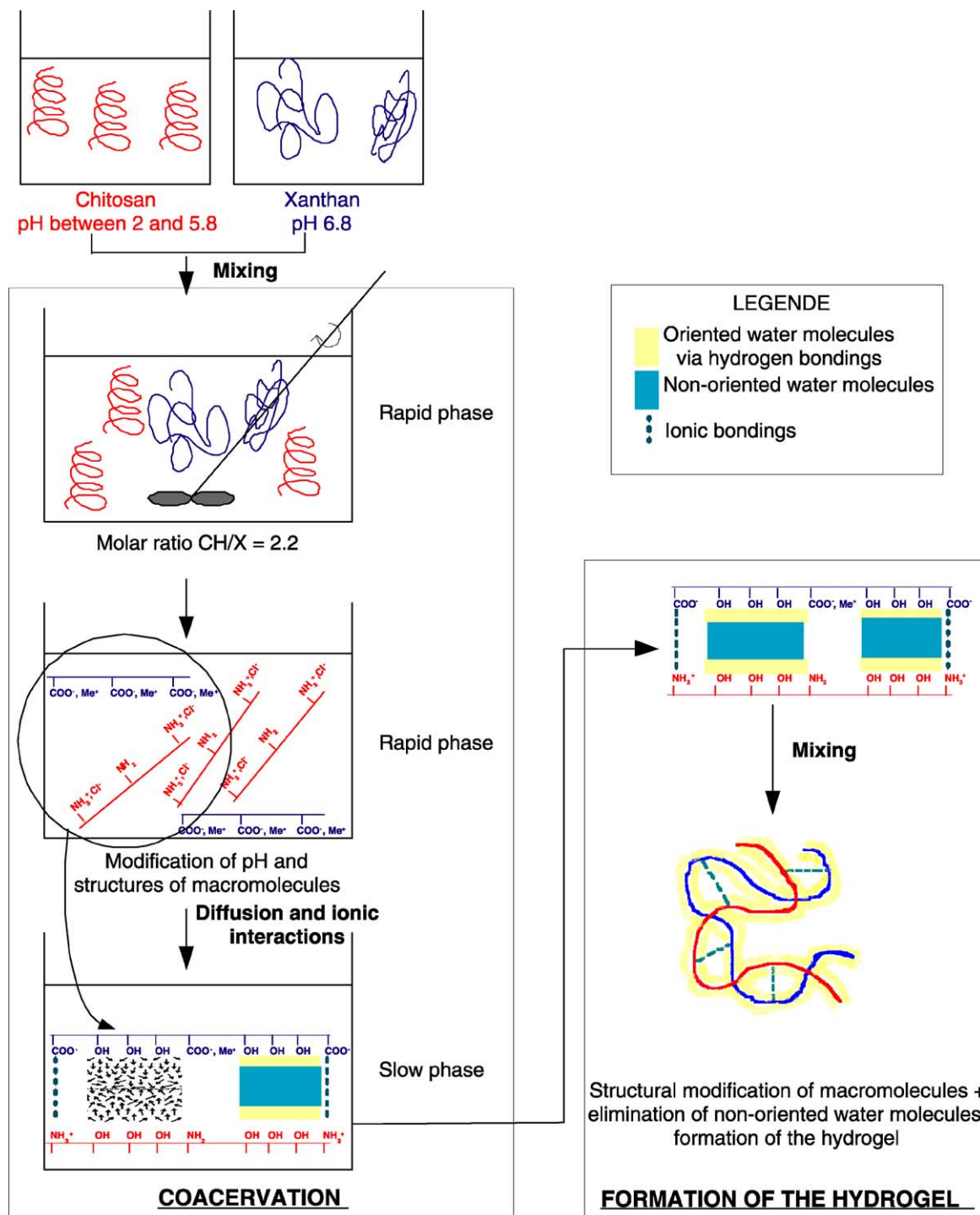


Fig. 1. Schematic illustration of the formation of the matrix: the coacervation and the formation of the hydrogel.

solutions of chitosan and xanthan were prepared as described in the previous study (Dumitriu et al., 1994). An aqueous solution of chitosan of 0.65 wt% is used. The pH of the solution of chitosan was varied between 2 and 5.8.

The molecular weight of chitosan has been determined by two methods: a viscometric method (Roberts & Domszy, 1982) and a gel permeation chromatographic (GPC) method (Jshizawa, 2002). For the viscometric method, chitosan

solutions of 0.1% (w/v) were prepared in 0.1 M CH<sub>3</sub>COOH/0.2 M NaCl and filtered. Viscosities were measured using a capillary Ubbelohde viscometer No. 1 B252, immersed in a thermostated water bath (Roberts & Domszy, 1982). The Mark–Houwink relation (Eq. (1)), allows to determine the viscometric molecular weight

$$[\eta] = K_m \bar{M}_v^\alpha \quad (1)$$

where  $K_m$  and  $\alpha$  are empirical constants ( $K_m = 1.81 \times 10^{-3} \text{ cm}^3 \text{ g}^{-1}$  and  $\alpha = 0.93$ ).

For the GPC method, the chromatographic system comprised a  $300 \times 7.8 \text{ mm}^2$  PolySep-GFC-PLinear column (Phenomenex, USA), a Waters 600 Controller Pump with Rheodyne injector, a degassing device and a Waters 410 Differential Refractometer detector. The column temperature was kept at  $40^\circ\text{C}$ . The mobile phase was  $0.5 \text{ M CH}_3\text{COOH}/0.2 \text{ M CH}_3\text{COONa}$  (Terbojevich, Cosani, Focher, & Marsano, 1993).

DA is determined by the infrared (Domsy & Roberts, 1985) and by elemental analysis methods (Muzzarelli, Rocchetti, Stanic, & Weckx, 1997). The infrared spectra are obtained between  $4000$  and  $400 \text{ cm}^{-1}$  with a Nicolet 5DXB FTIR spectrometer. Sample disks were prepared by mixing a few milligrams of chitosan with KBr in a vibrating ball mill. The compaction is made with a hydraulic press (Domszy & Roberts, 1985). The DA is determined by the ratio of N-acetyl groups (absorbance of the amide band at  $1655 \text{ cm}^{-1}$ ) and the hydroxyl group band (absorbance at  $3450 \text{ cm}^{-1}$ ). A fully N-acetylated chitosan gives a DA of 1.33, therefore, the DA is obtained using Eq. (2)

$$\text{DA} = \frac{A_{1655}}{A_{3450}} \frac{100}{1.33} \quad (2)$$

Elemental analysis measures the content of carbon, nitrogen and hydrogen in a given sample. The percent of nitrogen in chitosan can be used to calculate DA. Eq. (3) allows to calculate the DA: 8.695 corresponds to a fully deacetylated chitosan and 1.799 is the difference between 8.695 and 6.896 (percent of nitrogen, N, in fully acetylated chitin). A CHN Perkin Elmer 240 is used to carry out the elemental analysis of chitosan

$$\text{DA} = \frac{(8.695 - \text{N in wt\%}) \times 100}{1.799} \quad (3)$$

Pharmaceutical grade of xanthan was provided by Monsanto Pharmaceutical Ingredients. An aqueous solution of xanthan 0.65 wt% was used for the complexation. Three batches of xanthan with different percent of acid pyruvic (4.8, 3.2 and 2.8%) have been tested. The percent of pyruvic acid has been determined by Monsanto Pharmaceutical Ingredients.

## 2.2. Hydrogel preparation

*Preparation of the hydrogel in bulk.* Six litres of chitosan solution (0.65 wt%) and 8 l of xanthan solution (0.65 wt%) were mixed in a container ( $h = 64 \text{ cm}$  and  $\varnothing = 40 \text{ cm}$ ) with centred three-blade mixer. Agitation was conducted at room temperature for 5 min in order to obtain a gelatinous mass. At the beginning, the rotation rate is 950 rpm and at the end it is 750 rpm due to the increase of viscosity of the system. The resulting coacervate was decomposed after 0, 4 or 24 h with centred three-blade mixer at 1200 rpm in order to separate the surplus of water from the hydrogel ( $\cong 85\%$  of

water). The excess water is eliminated by filtration. To remove the excess of free chitosan, several washing/filtration cycles were needed. The hydrogel was freeze-dried and stored. Polyionic complex composed with chitosan and xanthan prepared in bulk can be reduced, if desired, to a fine powder by mechanical grinding. We used a 14 Fritzch grinder operating at 10,000 rpm.

*Preparation of the hydrogel in form of spheres.* Hundred millilitres of the solution of xanthan (at concentrations between 0.65 and 1 wt%), previously degassed were added, dropwise, with a syringe, into 200 ml of the solution of chitosan. The complexation reaction takes place under mild agitation (100–150 rpm) for 24 or 48 h at room temperature and the hydrogel spheres are formed. The latter were then washed with water to eliminate the excess free chitosan. The small spheres were freeze-dried and stored.

## 2.3. Determination of the swelling degree

The swelling degree was determined by placing 0.2 g of freeze-dried hydrogel in a centrifuge tube with 30 ml of water or buffer. The tube was turned upside down to wet the hydrogel. After 4 h, the hydrated hydrogel was separated of the excess of water by centrifugation (IEC HN-SII centrifuge) at 3600 rpm during 20 min. The increase of weight was due to that of water. The swelling degree ( $\alpha$ ) is determined via Eq. (4). Reported values are average of three measurements, and the root mean square standard deviation between measurements is reported as the relative standard uncertainty

$$\alpha = \frac{\text{weight}_{(\text{hydrated})} - \text{weight}_{(\text{dry})}}{\text{weight}_{(\text{dry})}} 100 \quad (4)$$

## 2.4. Rheological measurements

Rheological measurements were performed at  $20^\circ\text{C}$  with two controlled stress rheometers (Carri-Med CSL 100 and TA Instruments AR2000) in cone-plate geometry. Two cones with the same angle ( $4^\circ$ ) were used; their diameters were 2 and 4 cm, respectively. Measurements carried on with the two cones on the same systems gave comparable results. This was taken as an indication that wall effects ('apparent wall slip') did not affect the measurements. The possibility of true slippage, which produces erratic readings due to 'stick-slip' phenomena, was reasonably ruled out since consistent results were obtained. True slippage could be indeed a problem in the case of systems prone to syneresis, as it is the case for our hydrogels. After chitosan and xanthan have been mixed, the samples were placed in the measuring device and covered with a layer of low viscosity paraffine oil in order to avoid water evaporation. The evolution of the samples was monitored during 24 h by measuring the storage ( $G'$ ) and loss ( $G''$ ) moduli at 0.1 Hz

under 1% strain amplitude. After 24 h, the changes in the rheology of the systems became slow enough to allow the mechanical spectra to be recorded. The mechanical spectra were recorded over the 0.06–600 rad/s frequency range under 1% strain amplitude; the time needed to record one spectrum was about 1 h.

### 2.5. Microscopy characterization

The darkfield optical microscope (Leica Optoplan) with transmitted light was used for observation of the spheres. No preparation was necessary to observe the surface of the beads.

Transmission electron microscopy (TEM) samples have been cryoprepared: the small beads of hydrogel were put in liquid nitrogen and freeze-dried. The beads were included into an epoxy resin. Ultra-thin sections of 750 Å were made with ultra-thin microtome (LKB 8800) and examined under a Hitachi H-7500 transmission electron microscope without any contrast improving materials.

Scanning electron microscopy (SEM) samples were also cryoprepared (as per the TEM sample). The freeze-dried samples were fixed on an aluminium sample holder with a carbon-based adhesive tape. The samples were coated with Au–Pd. Samples were observed with a JEOL JSM-840A scanning electron microscope and with a Hitachi S-3000N.

### 2.6. Study of particles size

The analysis of particle dimensions was made by optical microscopy with dark background. Twenty photographs were made and all the particles in these photographs were analysed using the software package Sigma Scan Pro. The area, the perimeter, the Feret's diameter and the sphericity factor of particles were determined.

The Feret's diameter allows to quantify the degree of skewness of a particle population from its cumulative percent frequency distribution curves. The interquartile coefficient of skewness (IQCS) can be determined as shown in Eq. (5)

$$\text{IQCS} = \frac{(c - a) - (a - b)}{(c - a) + (a - b)} \quad (5)$$

where  $a$ ,  $b$  and  $c$ , are respectively, the median diameter, the lower quartile point and the upper quartile point.

The degree of symmetry of a particle size distribution can be quantified as the kurtosis. This symmetry is based on a comparison of the thickness of the tails and the sharpness of the peaks with those of a normal distribution. The coefficient of kurtosis ( $k$ ) can be determined as shown in Eq. (6)

$$k = \frac{n \sum (x - \bar{x})^4}{(\sum (x - \bar{x})^2)^2} - 3 \quad (6)$$

with  $x$ , the diameter of each particle,  $\bar{x}$ , the mean particle diameter and  $n$ , the number of particles.

## 3. Results and discussion

### 3.1. Characterization of the chitosan

Table 1 shows the molecular weight of three chitosans, as determined by the viscometric and GPC methods. Pullulan was used to make the calibration curve in the case of GPC (Jshizawa, 2002). The chromatographic results were in agreement with the viscosity-average molecular weights.

Table 2 presents the DA of three chitosans, as determined by the infrared method and elemental analysis. The two methods provide results that show good agreement.

### 3.2. Influence of pyruvic acid of xanthan on the complexation

As shown in Table 3, the percent of pyruvic acid of xanthan influences the percent of complexation and absorption properties ( $\alpha$ ). It is possible to see, that an increase of the percent of pyruvic acid of xanthan, increases the percent of complexation. The pyruvic acid of xanthan is on the lateral chain of this biopolymer and confers a negative charge. Therefore, an increase of the percent of pyruvic acid increases the global negative charge and allows an increase of the reticulation density. Consequently, the increase of pyruvic acid on xanthan allows a decrease of the absorption property ( $\alpha$ ) of this matrix.

### 3.3. Study of the swelling degree of the complex chitosan–xanthan

In the case of the preparation of the hydrogel in bulk, several key parameters influence the swelling degree of this matrix. Fig. 2 shows the influence of the time of the coacervation (steps 2 and 3, Fig. 1) for two molecular weights of chitosan. When the time of coacervation increases, the swelling degree of the matrix decreases. This result can be related to the diffusion of the

Table 1  
Molecular weights of chitosan

Chitosan sample	CH 79	CH 71P	CH V
Mv	600,000	1,000,000	1,000,000
Mn	200,167	357,757	471,949
Mw	766,410	977,866	1,071,922
I	3.83	2.73	2.27

Mv: molecular weight determined by viscometric method; Mn: number-average molecular weight determined by GPC method; Mw: weight-average molecular weight determined by GPC method; I: polydispersity index.

Table 2  
Degree of acetylation of chitosan

Chitosan sample	CH 79	CH 71P	CH V
DA (IR, %)	18	17	24
DA (EA, %)	18	16	27

macromolecular chains of chitosan and xanthan. Macromolecules of chitosan and xanthan diffuse slowly; therefore the longer the time of reaction, the higher the intermixing between chitosan and xanthan, resulting in an increased probability of interaction between  $-\text{NH}_3^+$ ,  $\text{Cl}^-$  of chitosan with  $-\text{COO}^-$ ,  $\text{Me}^+$  ( $\text{Me}^+$  indicates cation) of xanthan: in short, the connectivity between chitosan and xanthan increases creating a more compact structure that swells less.

The molecular weight of chitosan also influences the swelling degree. In this work, two molecular weights of chitosan have been used: 1,000,000 and 600,000. For zero time of coacervation, the swelling degree of this hydrogel is higher with the chitosan having MW of 600,000. At  $t = 0$ , there was not enough time for the diffusion of macromolecules into the system. The chitosan having the MW of 1,000,000 is more unstable than the chitosan with lower MW at pH 6.8 (the pH of the system during the coacervation), so the precipitation of the chitosan with a MW of 1,000,000 is more important. Therefore, the swelling degree of this polyionic complex made with the chitosan of MW 1,000,000 is smaller. But after 4 h of coacervation, it is the opposite. The chitosan with the molecular weight of 1,000,000 diffuses more slowly than the chitosan having a molecular weight of 600,000. The chitosan having a molecular weight of 600,000 can react well because its diffusion is greater. Thus, the swelling degree of the hydrogel made with chitosan having a molecular weight of 600,000 decreases rapidly and become smaller than the swelling degree of the hydrogel made with chitosan having a molecular weight of 1,000,000. It is possible to see that the swelling degree of the hydrogel made with chitosan having a molecular weight of 1,000,000 decrease but more slowly than that made with chitosan having a molecular weight of 600,000.

The pH of the solution of chitosan plays a fundamental role on the swelling degree of this matrix as shown in Fig. 3. For a pH comprised between 3.5 and 5.8, the swelling degree of the hydrogel increases with the pH of the solution

Table 3  
Influence of the percent of pyruvic acid of xanthan on the complexation

Xanthan: percent of pyruvic acid	Percent of complexation	Swelling degree (%)
2.8	50	6000
3.2	60	3000
4.8	72	350

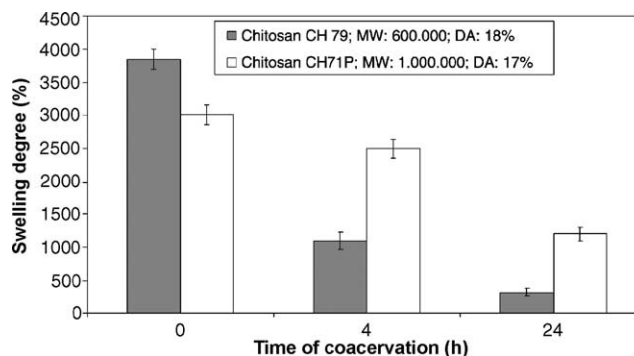


Fig. 2. Influence of the time of coacervation and of the molecular weight of chitosan on the swelling degree. The solution used to swell the matrix is distilled water and the pH of the solution of chitosan used to make the matrix is 5.6.

of chitosan. The pH governs the number of amine groups as a salt ( $-\text{NH}_3^+$ ,  $\text{Cl}^-$ ) on the macromolecule of chitosan. When the pH of the solution of chitosan increases, the number of  $-\text{NH}_2$  increases and the number of  $-\text{NH}_3^+$ ,  $\text{Cl}^-$  decreases resulting in a decrease of the probability of interaction between  $-\text{NH}_3^+$ ,  $\text{Cl}^-$  of chitosan and  $-\text{COO}^-$ ,  $\text{Me}^+$  of xanthan and thus a decrease on the number of connections between chitosan and xanthan. In Fig. 3, it is also possible to see the effect of a very acidic pH (pH = 2) of the solution of chitosan. The swelling degree is very high due to the excess of free HCl (HCl not associated with chitosan). In this case, the matrix swells very well. This effect is also noticed in Fig. 5 where the pH of the solution used for swelling is 1.5.

In Fig. 4, the effect of the pH of the swelling solution on the swelling degree of this hydrogel is shown: in strongly acidic media, the hydrogel swells more than in media at pH comprised between 3.1 and 5.5. However, it is with increasing basicity that swelling is more pronounced. When the solution used for swelling has a pH comprised between 3.1 and 4.8, an increase in pH corresponds to

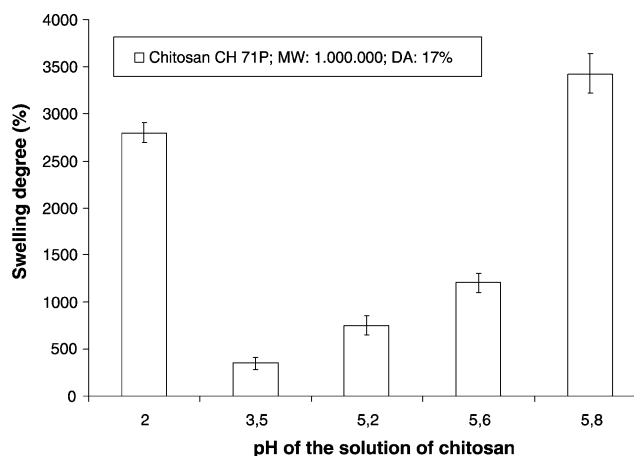


Fig. 3. Influence of the pH of the solution of chitosan on the swelling degree of the matrix. The solution used to swell the matrix is distilled water.

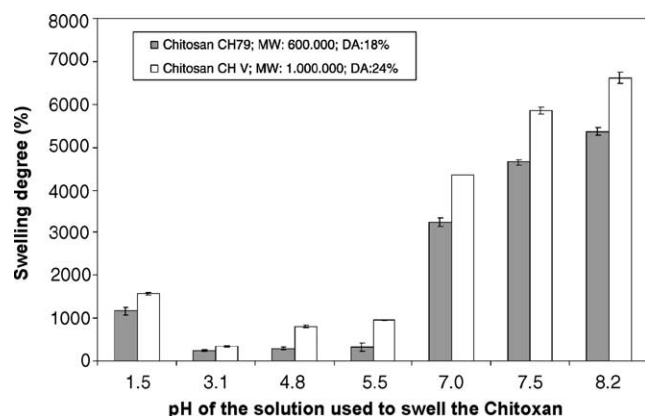


Fig. 4. Effect of the pH of the swelling solution on the swelling degree of the matrix for two molecular weights of chitosan.

a decrease in the concentration of  $H^+$ ,  $A^-$  in the solution with a concomitant decrease in  $-NH_3^+$ ,  $A^-$  coupling in the number of connectivity links. In the case of basic media, when the pH increases, the number of  $Me^+OH^-$  increases in the solution used to swell.  $Me^+OH^-$  can interact with  $-NH_3^+$ ,  $Cl^-$  of chitosan and form  $-NH_2$  and  $H_2O$  as well as  $Me^+$ ,  $Cl^-$ . A decrease in the connectivity results in increased swelling.

Fig. 5 shows the results of the study on the swelling of the hydrogel in form of spheres. Fig. 5A and B show, respectively, the effect of the time of coacervation with solutions of xanthan at 0.65 and 1 wt%. The same effects have been found for spheres as for bulk preparation. The time of coacervation influences the swelling degree: the longer the time, the lower the swelling degree. Also, the pH of the solution of chitosan influences the swelling degree. The explanation of these effects have been provided when commenting on the results of Fig. 2. Fig. 5C compares the swelling characteristics of bulk and spheres preparation. At the same conditions of preparation, the spheres swell more than the bulk preparation. This phenomenon can be explained by the rapid formation of a membrane. During the time of coacervation, the chitosan must diffuse through the bead membrane and interact with the xanthan. The membrane decreases the rate of diffusion of chitosan and it is quite possible that some macromolecules of xanthan have not interacted with chitosan. Thus, beads of hydrogel swell more than bulk hydrogel preparation.

### 3.4. Rheological monitoring of coacervation kinetics

During coacervation, the rheology of the system shift from that of a predominantly viscous liquid to that of a strongly viscoelastic solid-like material (Kobayashi, 2001). This is shown on Fig. 6, which shows the variation with time of the storage modulus of the coacervates. Measurements started immediately after mixing and they reflect the evolution of the system while polyionic interactions are developing between the two

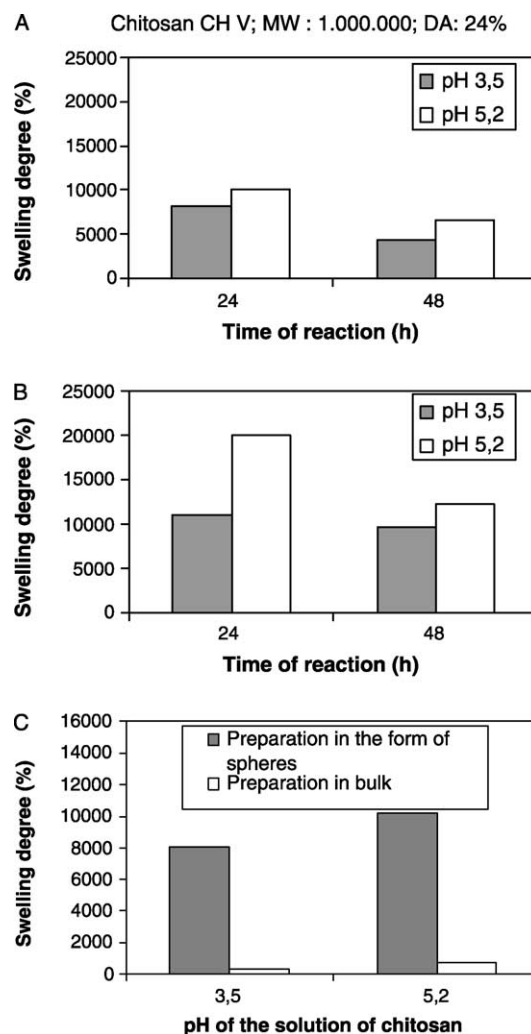


Fig. 5. (A) Effect of the time of coacervation and pH of the solution of chitosan on the swelling of beads made with a solution of xanthan at 0.65 wt%. (B) Effect of the time of coacervation and pH of the solution of chitosan on the swelling degree of beads made with a solution of xanthan at 1 wt%. (C) Comparison of the swelling degree of the hydrogel prepared in bulk and in form of beads (the concentration of the solution of xanthan is 0.65% and the time of coacervation is 24 h).

polysaccharides. During the first 4 h (phase I), one observes a steep increase of  $G'$ . This is followed by a second phase (phase II) during which the slope of curve of  $G'$  versus time decreases progressively. After 24 h, this slope has become very small, but  $G'$  still has not reached a plateau. This type of 'kinetics' is generally observed in the case of the physical (Clark, Richardson, Ross-Murphy, & Stubbs, 1989; Clark, Gidley, Richardson, & Ross-Murphy, 1983; Ross-Murphy, 1991) and chemical (Arguelles-Monal, Goycoolea, Peniche, & Higuera-Ciapara, 1998; Lin-Gibson, Walls, Kennedy, & Welsh, 2004) gelation of aqueous biopolymer systems. Classical treatment of dynamic data, as performed by the rheometers softwares, supposes that the response to the sinusoidal mechanical excitation is a sinusoidal signal with the same frequency, i.e. the dynamic measurements are

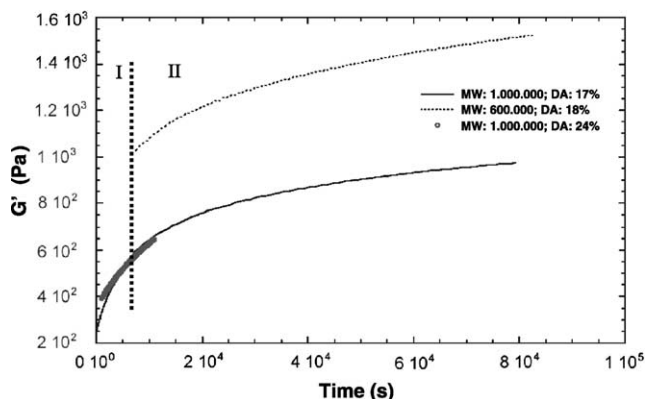


Fig. 6. Evolution of storage modulus versus time of coacervation. (frequency = 0.1 Hz; temperature = 20 °C).

performed within the linearity range of the material. This is usually the case if the strain amplitude is kept low enough, and the linearity limit is generally determined by performing the measurements at increasing strain amplitude values. Such a procedure cannot be followed in the case of 'kinetic' experiments since the material is constantly changing with time. On the other hand, and precisely for the same reason, the problem of linearity is then especially delicate. Since the systems behave linearly, or nearly so, at 1% strain amplitude in all its pseudoequilibrium states, as it will be shown later, we have supposed that the linearity condition was fulfilled all along the paths leading from initial to final states during monitoring experiments. Anyway, such experiments at fixed frequency on complex systems convey little rheological information; they are just convenient means to track structural changes occurring in the material. In such conditions, the linearity issue is not so critical provided the strain amplitude is kept low in order that possible departure from linearity remains small and that shearing does not interfere with the processes that are monitored. The same data are plotted in Fig. 7 in terms of  $\tan(\delta) = G''/G'$  versus coacervation time. This plot delineates clearly the two phases. During phase I,  $\tan(\delta)$  decreases steeply, showing the increase in the viscoelastic character of the system, and then reaches a minimum (Chitosan MW 1,000,000, DA 17%) or a plateau value (Chitosan MW 600,000). During phase II,  $\tan(\delta)$  increases slightly before reaching a plateau in the case of the higher MW chitosan sample, whereas it remains practically constant in the case of the lower MW chitosan sample with a similar DA.

Measurements at one fixed frequency such as those of Figs. 6 and 7 do not lend themselves to unambiguous interpretation, since the results depend on the choice of the frequency and since they do not describe actually the changes in the viscoelastic behaviour of the system. This would require the mechanical spectrum to be recorded at intervals during the coacervation reaction. But this is not practically feasible using classical dynamic rheological measurements since the rheology of the material would

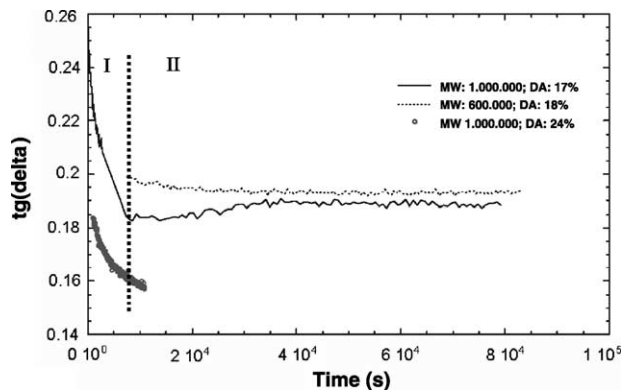


Fig. 7. Evolution of the loss tangent versus time of coacervation. (frequency = 0.1 Hz; temperature = 20 °C).

change during the time necessary to record the mechanical spectrum (1 h). It seems, however, reasonable to consider that phase I corresponds essentially to the formation of the network, a process which takes about 4 h because, as already explained, it requires diffusion and structural matching of the two macromolecular species. At the end of this phase, a network is formed and any subsequent changes in the system would become much slower because the rigidification of the system decreases the mobility and the flexibility of the macromolecules. During phase II, the gel formed during phase I would strengthen slowly through structural rearrangements at a local scale, hence the continuing increase in  $G'$  continues but without appreciable qualitative modification of its viscoelastic behaviour since  $\tan(\delta)$  remains practically constant. It is interesting to observe that for DA 17%, the chitosan with the higher molecular weight shows  $G'$  values which are at all times lower than the chitosan with the lower MW, whereas the values of  $\tan(\delta)$  for the two systems are rather close to each other. The density of rheologically effective crosslinks seems thus lower at any stage of the coacervation process in the case of the former system.

### 3.5. Rheological monitoring of the evolution of hydrogels with time

Hydrogels prepared by mechanical mixing of the coacervates are practically stable systems as far as it can be concluded from the records of  $G'$  measured at 0.1 Hz as a function of time. Figs. 8 and 9 show that  $G'$  do not change appreciably with time for hydrogels prepared after zero time of coacervation as well as after 24 h of coacervation. The latter give higher  $G'$  values than the former. For chitosans with the same DA of 17%, the hydrogel prepared with MW 600,000 sample gives a higher  $G'$  value than that of the MW 1,000,000 sample after zero coacervation time, as was the case for  $G'$  of the coacervates, but the situation is reversed for the hydrogels when prepared after 24 h coacervation time.

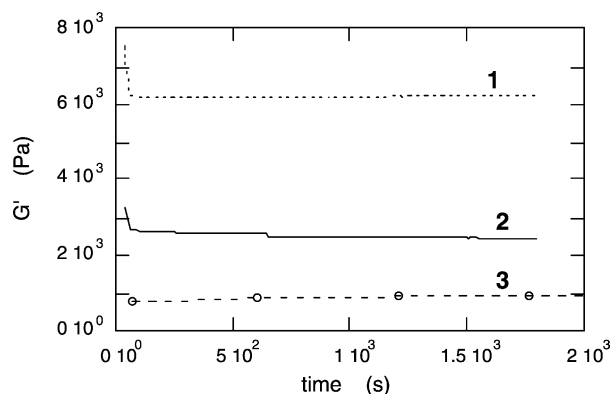


Fig. 8. Evolution of the storage modulus versus time for hydrogels prepared after a zero time of coacervation. (frequency = 0.1 Hz; temperature = 20 °C).

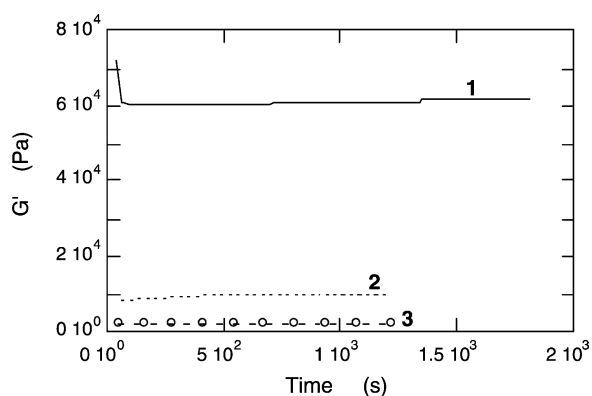


Fig. 9. Evolution of the storage modulus versus time for hydrogels prepared after a time of coacervation of 24 h. (frequency = 0.1 Hz; temperature = 20 °C).

The mechanical mixing process induces structural modifications within the coacervates and the elimination of a fraction of the water (non-oriented water). The latter effect amounts to an increase in the macromolecular concentration of the gels as compared to the coacervates, and it is therefore the main factor responsible for the higher  $G'$  values observed for the gels as compared to the coacervates. For the hydrogels prepared from the MW 600,000 and the MW 1,000,000 chitosan samples after zero or after 24 h coacervation time,  $G'$  varies in the same direction as the swelling factor, as indicated by the comparison of Figs. 8 and 9 with Fig. 2 and the data of

Table 4. The trend is however reversed when comparing the hydrogels prepared after zero and after 24 h coacervation time from the same chitosan sample (Table 4). The explanation could be the same as that given for the effect of MW on the swelling degree (Section 3.2).

### 3.6. Viscoelastic behaviour of the coacervates and of the gels

After 24 h reaction time, the evolution of the coacervates becomes slow enough to allow the mechanical spectra to be recorded (Fig. 6). Fig. 10A shows the mechanical spectra of the coacervates after 24 h reaction time obtained with the chitosan samples with DA 17% and MW 600,000 and 1,000,000. On the same figure, the spectrum of the coacervate prepared with the DA 24% MW 1,000,000 chitosan sample recorded after 4 h reaction time is plotted for comparison. After 4 h, the coacervate is still evolving relatively fast; its viscoelastic properties are changing during the time necessary to record the spectrum. This affects mainly the data in the lower frequency region and explains the unphysical increase observed for  $G'$  as the frequency decreases in this region of the spectrum. This problem is not met in the case of the hydrogels, which show pseudoequilibrium in all cases as we have already stressed it. The mechanical spectra of the hydrogels are shown in Fig. 10B (hydrogels prepared after zero coacervation time) and C (hydrogels prepared after 24 h coacervation time). Mechanical spectra have no meaning unless they are recorded within the linearity domain of the viscoelastic behaviour. Linearity implies that  $G'(w)$  and  $G''(w)$  are not independent functions, but are linked by the mechanical equivalents of Kronig–Kramers equations (Eq. (7)). A convenient first order approximation gives (Tschoegl, 1989):

$$G''(w) = \frac{\pi}{2} \frac{dG'(w)}{d \ln(w)} \quad (7)$$

Eq. (7) provides a convenient means to check that the data have been recorded within the linearity domain all over the frequency window. Since Eq. (7) is just a tractable approximation to the exact relationship between the storage and loss moduli function, on one hand, and since the direct numerical derivation of  $G'(w)$  data which was performed is very sensitive to minute accidents on the  $G'(w)$  curve, one cannot expect a strict coincidence of measured and calculated values of  $G''$ . Fig. 11 gives some examples

Table 4  
Swelling degrees and storage moduli of hydrogels

Time of coacervation	Chitosan	Swelling degree (%)	Storage modulus (Pa)
Without coacervation (0 h)	PM: 600,000; DA: 18%	3850	6140
Without coacervation (0 h)	PM: 1,000,000; DA: 17%	3010	2310
With coacervation (24 h)	PM: 600,000; DA: 18%	320	9620
With coacervation (24 h)	PM: 1,000,000; DA: 17%	1200	80,300

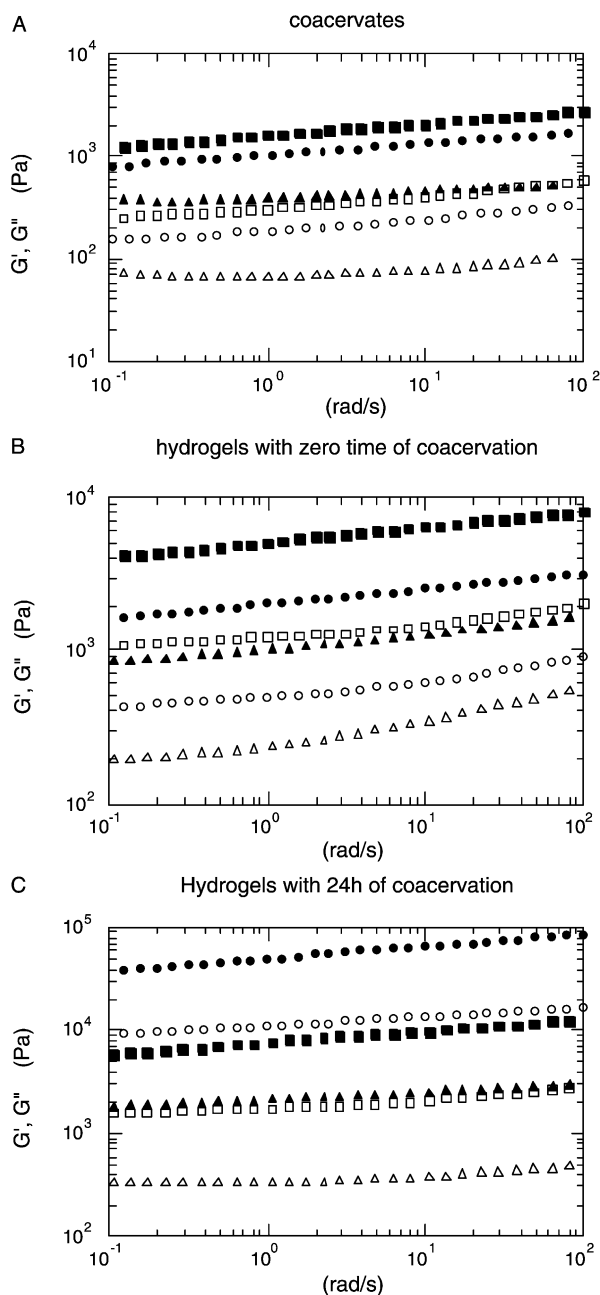


Fig. 10. Mechanical spectra for the coacervates (A), the hydrogels prepared with a time of coacervation of 0 h (B) and the hydrogel prepared with a time of coacervation of 24 h (C).

showing that Eq. (7) is reasonably verified by our data. All the spectra are qualitatively similar; they correspond to a section of the viscoelastic plateau, with  $G'$  showing a rather low dependence on the frequency and nearly ten times larger values than  $G''$ . Both moduli are fairly high all over the frequency window, particularly in the case of the hydrogels prepared after 24 h coacervation. Within the experimental frequency range, all systems behave as viscoelastic solids. Nevertheless, the possibility that they could flow at longer time (lower frequency) scales cannot be excluded.

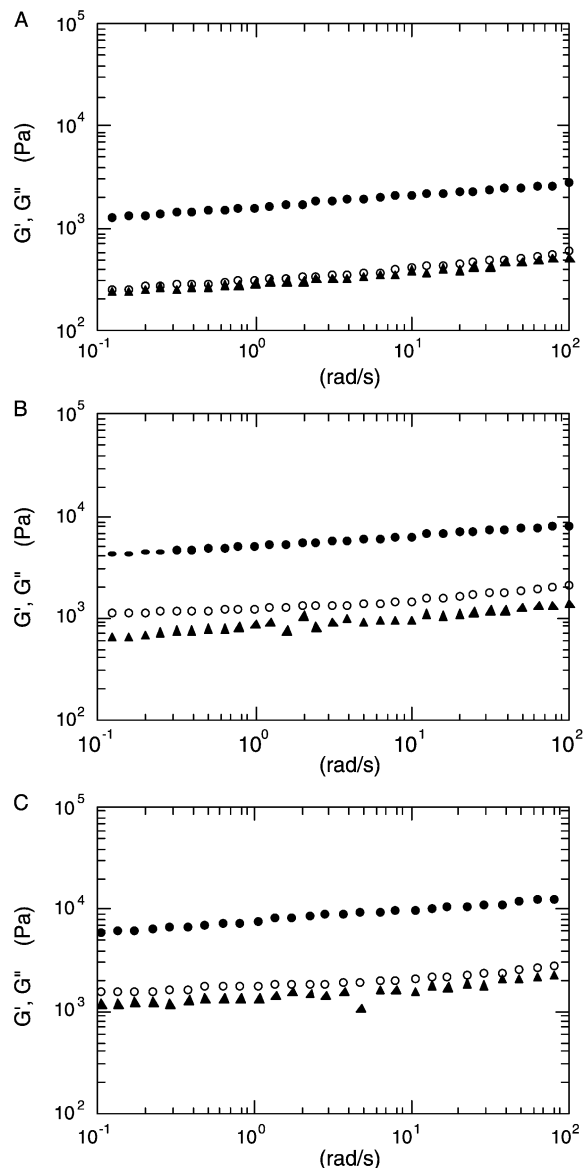


Fig. 11. Check of the linearity of the viscoelastic behaviour of the systems prepared with the MW 600,000 (DA: 18%) chitosan sample. Circles: experimental data (filled:  $G'$ , empty:  $G''$ ). Filled triangles:  $G''$  calculated with Eq. (7). (A) coacervate; (B) hydrogel prepared with zero coacervation time; (C) hydrogel prepared with 24 h coacervation time.

### 3.7. Microscopy characterization

A representative sphere of this matrix has been observed by optical microscopy. Fig. 12 shows the external structure of the bead. Since with optical microscopy no treatment is available to observe the bead, the original structure is observed. Fig. 12 shows a regular arrangement.

TEM has allowed the observation of ultra-thin sections of the sphere. In Fig. 13, it is possible to distinguish an interface. This interface is continuous and rather compact. In the inner part of bead, there is a porous network showing a fibrillar structure. The size of pores is estimated to be comprised between 100 and 250 nm.

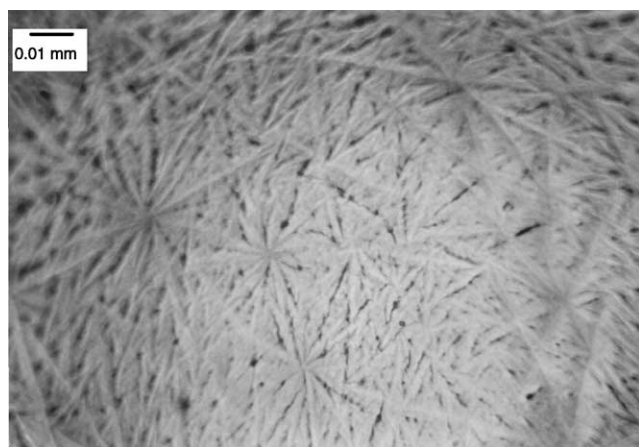


Fig. 12. Optical darkfield microscopy of the surface of a hydrated bead of hydrogel.

SEM has permitted the observation of the morphology of the external and internal structure of a bead of this matrix. Fig. 14 shows the observation zones. The external as well as the internal structures and the composition of a fiber (in a white rectangle) have been analysed.

Figs. 15 and 16 show the external structure of a sphere of this matrix at two magnifications. At low magnification, a regular pattern is observed (Fig. 15). Such regular pattern has already been observed via optical microscopy (Fig. 12) and has been enhanced by freeze-drying. At high magnification (Fig. 16), a porous network is clearly distinguished. In previous studies about immobilized enzymes into beads of complexes chitosan–xanthan (Dumitriu and Chornet, 1998b; Dumitriu et al., 1995b, 1994; Magnin et al., 2002,

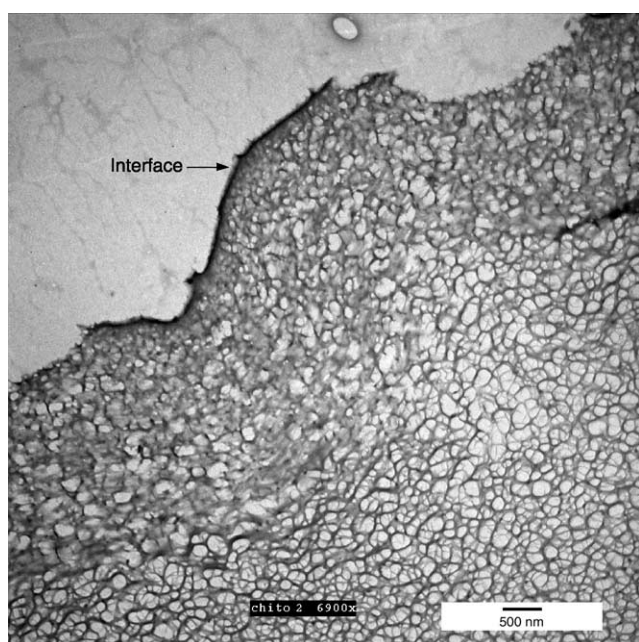


Fig. 13. Transmission electron microscopy of an ultra-thin section of a bead of hydrogel.

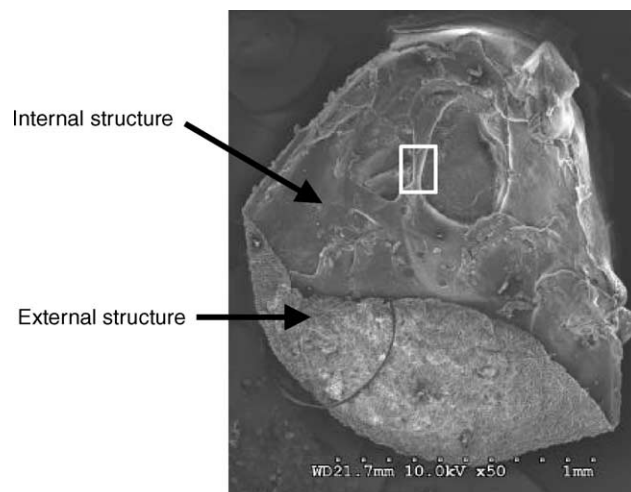


Fig. 14. Scanning electron microscopy of a bead of hydrogel.

2001), high activities have been found but no microscopic studies had shown the porosity of the external structure of the sphere. This porosity explains the diffusion of substrates and products. When this hydrogel is used as a matrix for drug delivery system, the control of the porosity likely influences the rate of drug release.

Fig. 17 shows the internal structure of a bead of this matrix. A porous network composed of fibres is observed. It is difficult to estimate the size of the pores from Fig. 17 due to the 3D network. The diameter of the fibres is inferior at  $1 \mu\text{m}$ .

### 3.8. Study of fine particles (i.e. powder) of complexes chitosan–xanthan

For some applications, such as transmucosal drug delivery system, the dimensions of particulate solids are important in achieving optimum application of efficient and

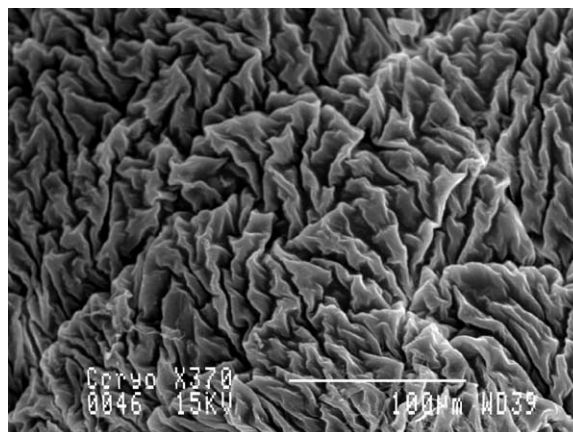


Fig. 15. Scanning electron microscopy of the external structure of a bead: a regular pattern is observed.

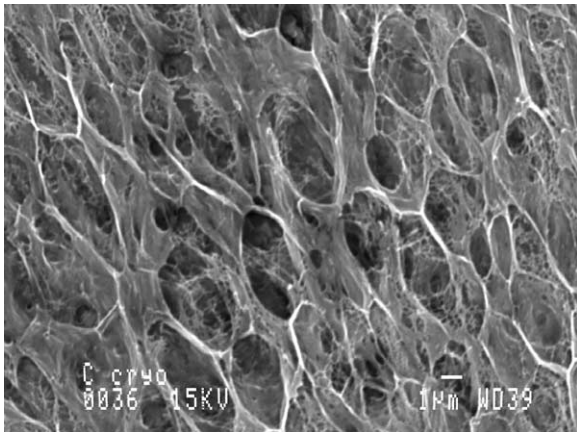


Fig. 16. Scanning electron microscopy of the external structure of a bead: a porous network is observed.

specific drugs (Staniforth, 2002). The particle size of the powder may influence the subsequent performance of the drug (Staniforth, 2002).

Figs. 18 and 19 show, respectively, a microphotography of dry particles and hydrated particles observed by optical microscopy. The rehydration of particles has been made directly on the blade of microscope with a syringe.

Figs. 20–23 show the distributions for dry (D) and hydrated (H) particles for area, perimeter, Feret diameter and sphericity factor. From Fig. 20, we can observe that there is a shift of the maximum of the area between dry and hydrated particles (factor of 10). This shift is also found for the Feret diameter (Fig. 22). It can be noticed that the sphericity factor is different for dry and hydrated particles (Fig. 23). For dry particles, the sphericity factor is comprised between 0 and 1 since the dry particles can be very angular. For hydrated particles this is not the case since the sphericity factors are between 0.6 and 1. Therefore, the swelling of particles increase their sphericity.

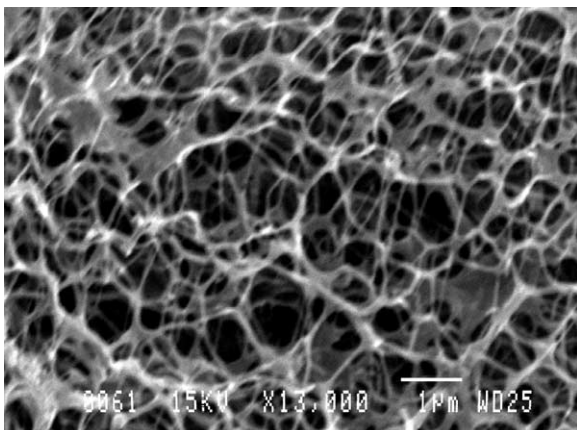


Fig. 17. Scanning electron microscopy of the internal structure of a bead: a fibrillar structure is observed.

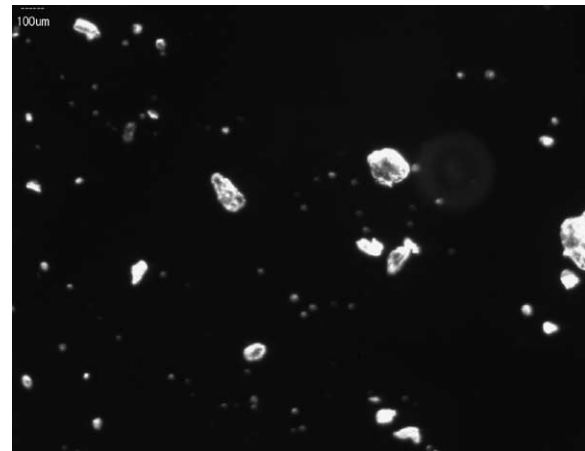


Fig. 18. Dry particles of this hydrogel observed by darkfield optical microscopy (transmitted light). 100 × .

The coefficient of skewness and the degree of symmetry of the particle size distribution have been determined by using, respectively, Eqs. (5) and (6). The IQCS have been determined from the cumulative percent frequency distribution curves presented in Fig. 22. The IQCS of dry and hydrated particles are, respectively, 0.34 and 0.21. IQCS can take any value between  $-1$  and  $+1$  and is equal to 0 in the case of a symmetrical size distribution. The values of 0.34 and 0.21 show an asymmetry between the quartile points in the two cases for dry and hydrated particles, and this asymmetry is more important for dry particles. The degrees of symmetry for dry and hydrated particles are 598 and 28. The coefficients of kurtosis have positive values for curves showing leptokurtic size distributions because the number of small particles are predominant.

Fig. 24 allows to see the distribution of dry particles versus their sphericity factor. The dry particles having a sphericity factor comprised between 0.8 and 1 and between

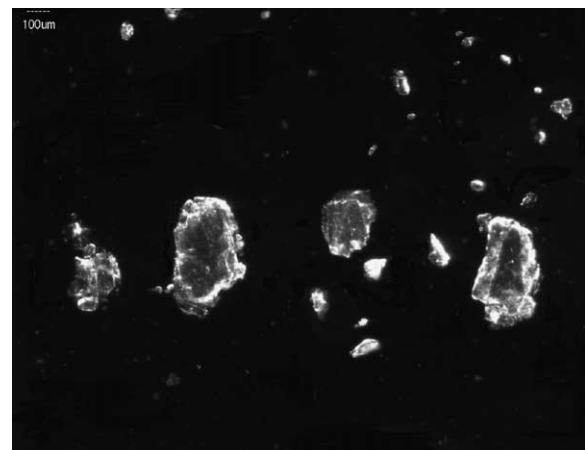


Fig. 19. Hydrated particles of this hydrogel observed by darkfield optical microscopy (transmitted light). 100 × .

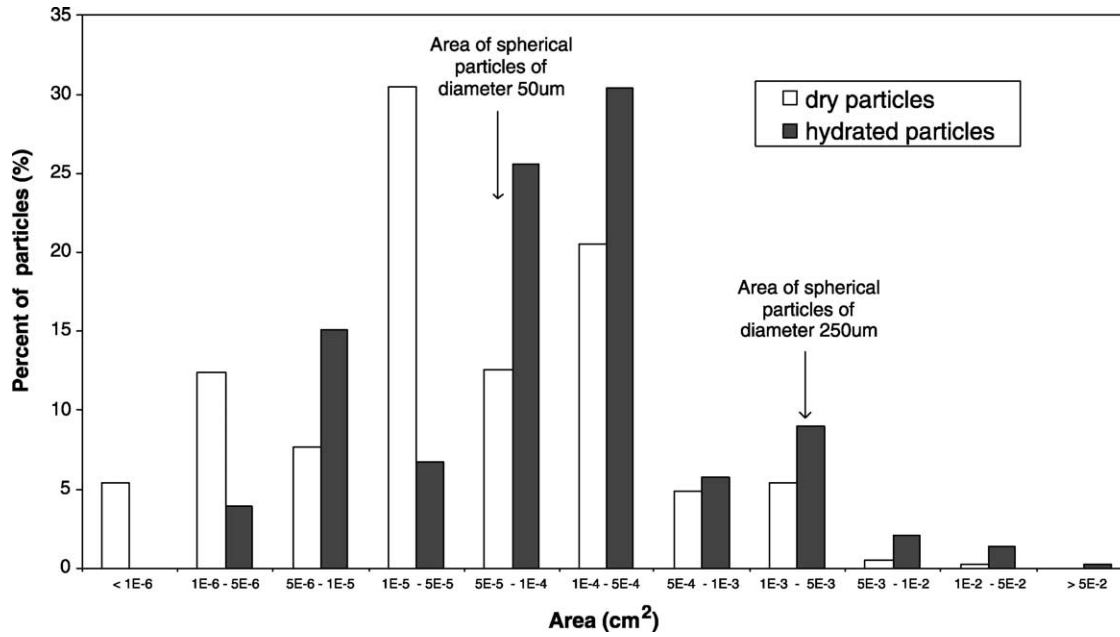


Fig. 20. Distribution of the area of dry and hydrated particle of this hydrogel.

0.6 and 0.8 represent the smallest size fraction. Particles having a sphericity factor between 0.4 and 0.6, represent the particles with a medium size. Finally, the larger particles have a sphericity factor between 0 and 0.4. The major part of the particles are acicular due to mechanical grinding. However, the smaller particles can be considered as spherical. During the grinding, the rotation of the knife can allow an erosion of acicular particles that explain

the presence of spherical particles. Moreover, the larger particles have a sphericity factor inferior to 0.4, thus they are filamentous.

#### 4. Conclusion

Physicochemical and structural methods have been used to characterize a potential matrix for pharmaceutical

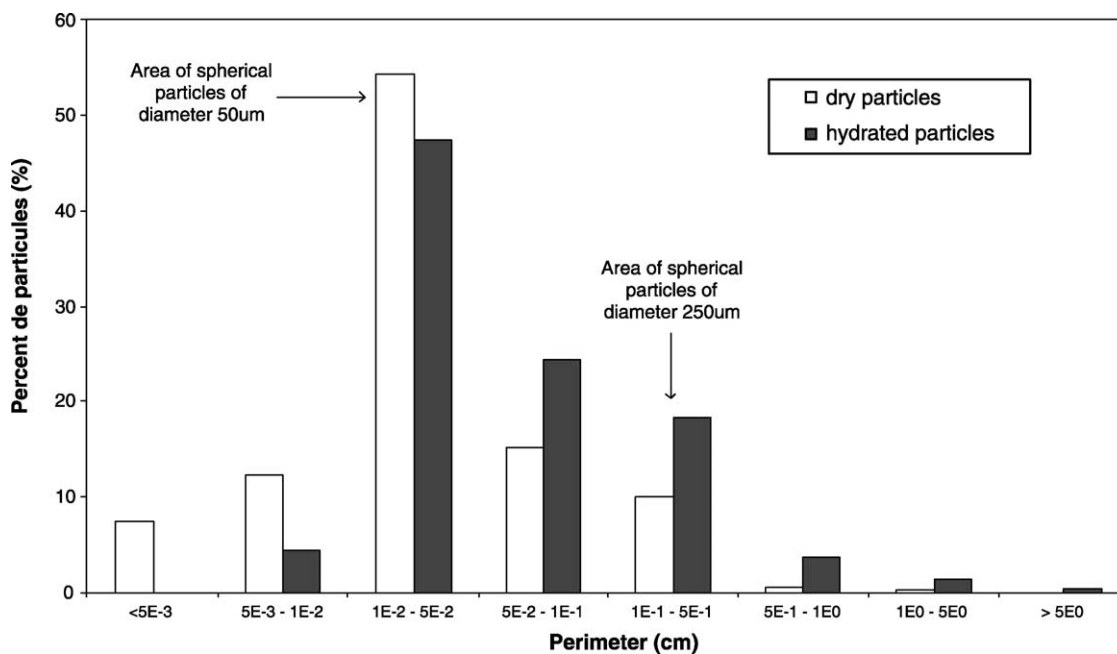


Fig. 21. Distribution of the perimeter of dry and hydrated particle of this hydrogel.

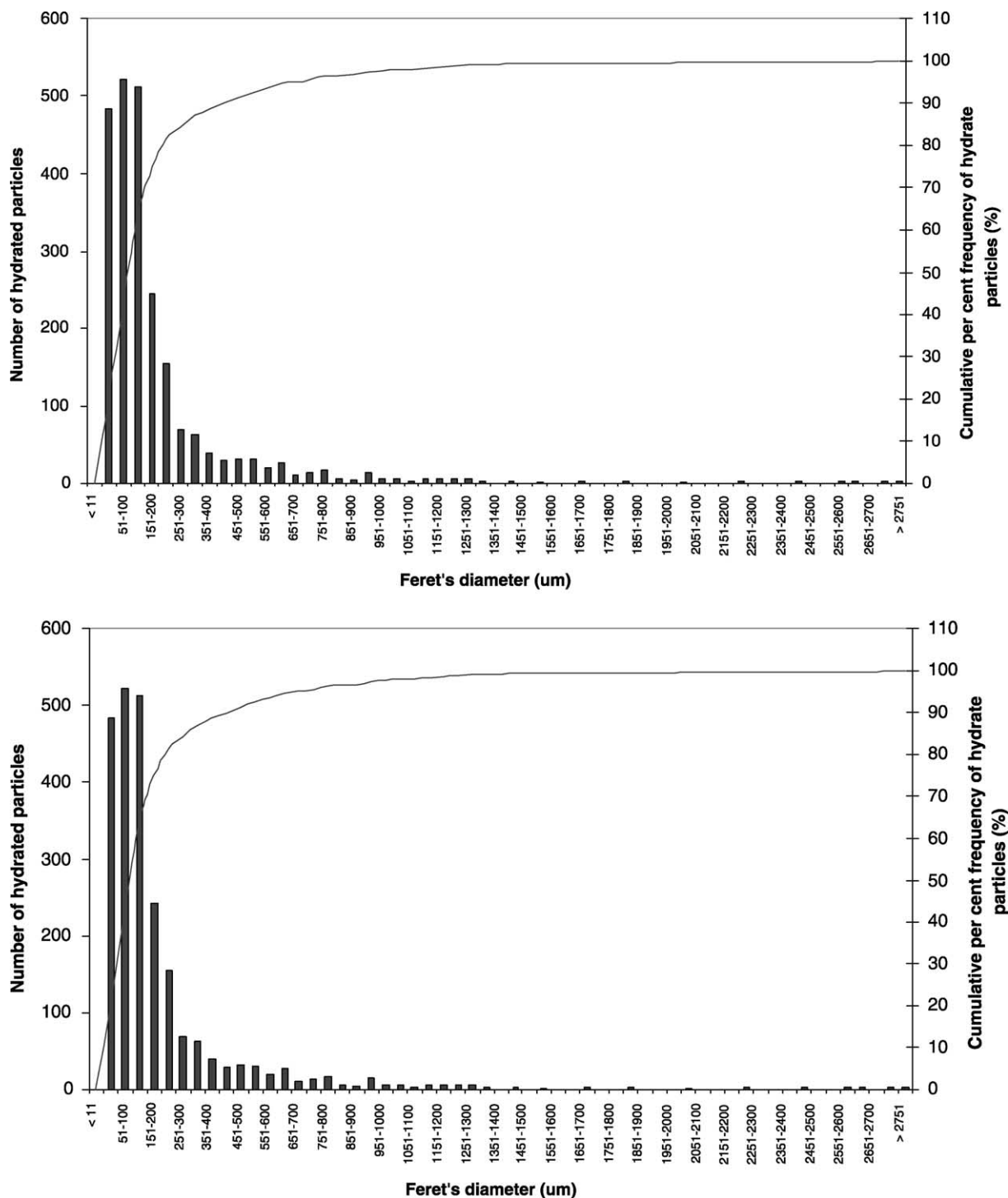


Fig. 22. Distribution of the Feret diameter of dry (a) and hydrated (b) particles of this hydrogel.

formulations and biotechnology applications. This hydrogel shows a swelling degree that can be easily modulated by the choice of the molecular weight and DA of chitosan, the pH of the solution of chitosan and the time of coacervation. The latter two parameters are very important and are operationally controllable. Moreover, it is possible to prepare this hydrogel in bulk or in the form of beads: these two forms of the hydrogel have swelling degrees, which can be varied

between 600 and 20,000%. This range of swelling degrees is desirable for using this matrix as vehicle for drug delivery systems since the swelling degree influence the rate of drug release.

This study also highlights that the swelling degree of this matrix is influenced by the pH of the solution used to swell the hydrogel. This information is important since in the case of drug administration via an oral route (the most frequently

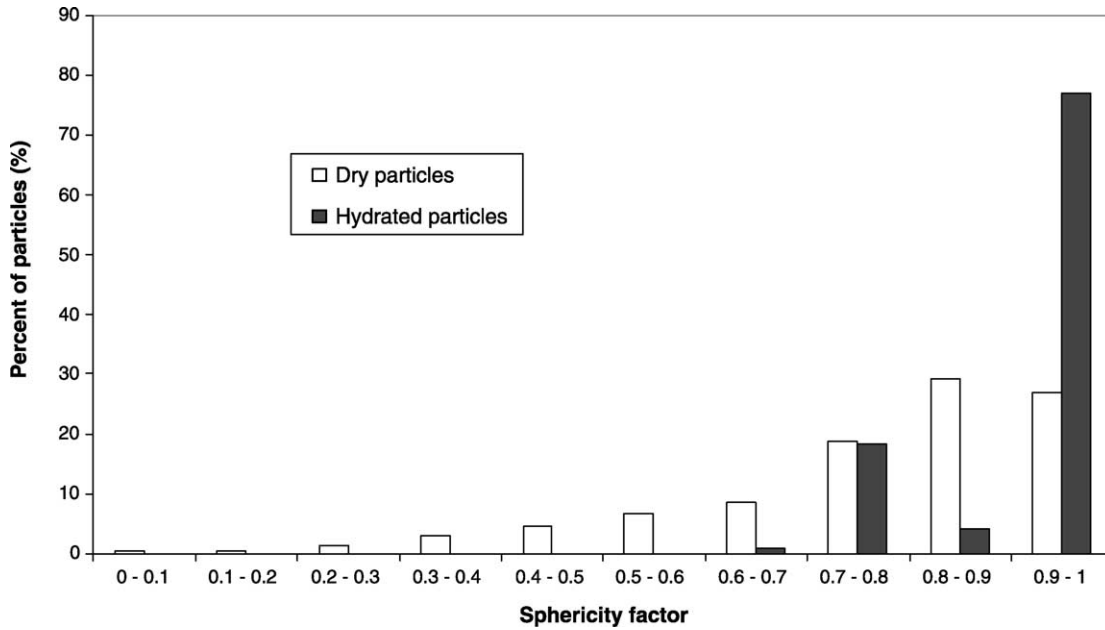


Fig. 23. Distribution of the sphericity factor of dry and hydrated particle of this hydrogel.

used), the pH of fluids vary considerably along the length of the gastrointestinal tract (1–3 in the stomach and 5–8 in the small intestine).

Rheological measurements have been used to understand the coacervation step and subsequent structural modifications to form the hydrogel. Such information is important

for the process of fabrication. The time of coacervation influences the swelling degree, and as well the rheological characteristics of the matrix. The kinetic curve clearly shows a classic sol–gel transition and the organization of the hydrogel in a ‘quasi-ordered’ network during the coacervation. After subsequent structural modification, by

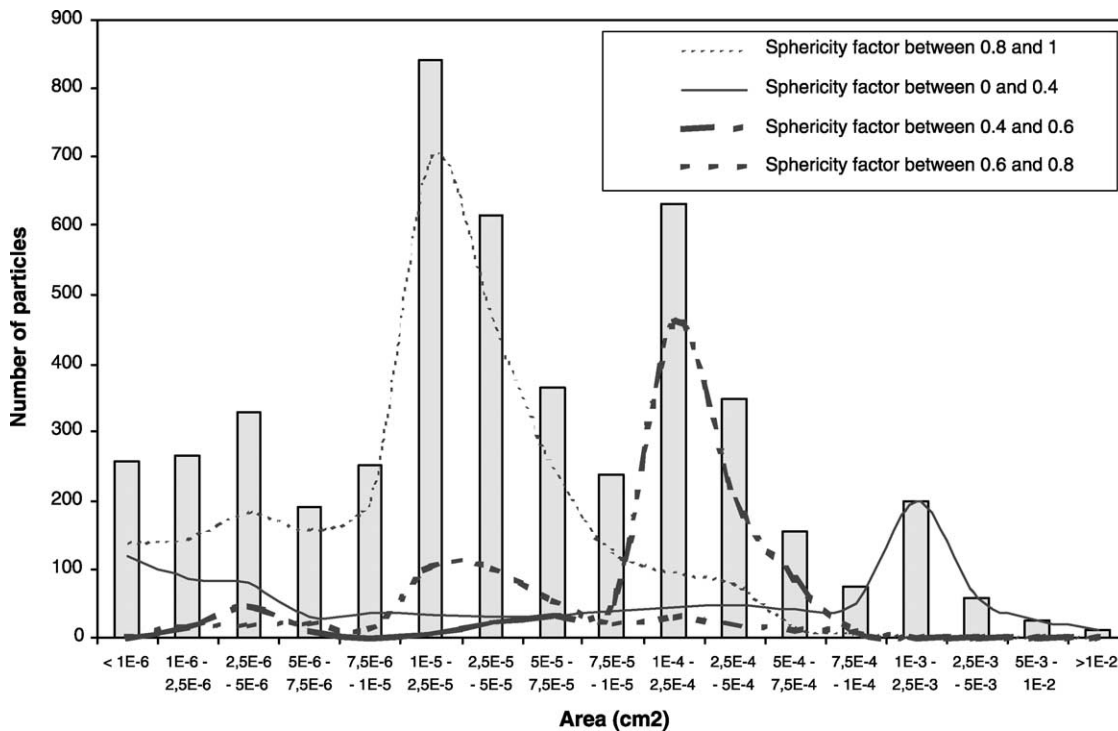


Fig. 24. Distribution of the area of dry particles of this hydrogel versus their sphericity factor.

mixing, the hydrogels show stable storage modulus with time and their mechanical rheological spectra have proven their solid-like behavior.

The method of preparation of the samples by cryopreparation has improved the quality of the sample and highlighted the structure and microstructure of this matrix. Microscopic investigations have shown that this hydrogel has a regular organization: a porous network composed of fibres. The size of pores has been estimated between 100 and 25 nm and the diameter of a fiber comprised between 1 and 10  $\mu\text{m}$ . The microstructure of the major fiber is composed of parallel microfibrils connected by lateral fibrils.

The particulate solids obtained by mechanical grinding of bulk hydrogel show a sphericity factor that varies between 0.016 and 1. The area, perimeter and Feret diameter have been determined. A range comprised between 5 and 12,500  $\mu\text{m}$  can be obtained. Mechanical grinding of this hydrogel thus permits to obtain a suitable diameter powder for pharmaceutical applications.

It can be concluded from the data presented in this paper, that this hydrogel is an appropriate matrix for pharmaceutical formulations and for biotechnological applications due to its favourable physicochemical properties.

## Acknowledgements

Financial support from NSERC (Natural Sciences and Engineering Research Council of Canada) is gratefully acknowledged.

## References

- Arguelles-Monal, W., Goycoolea, F., Peniche, C., & Higuera-Ciajara, I. (1998). Rheological study of the chitosan/glutaraldehyde chemical gel system. *Polymer Gels and Networks*, 6, 429–440.
- Brinker, C. J., & Scherer, G. W. (1990). In H. B. Jovanovich (Ed.), *Sol–gel sciences: the physical and chemistry of sol–gel processing*. San Diego: Academic press.
- Clark, A., Gidley, M., Richardson, R., & Ross-Murphy, S. (1989). Rheological studies of aqueous amylose gels: the effect of chain length and concentration on gel modulus. *Macromolecules*, 22, 346–351.
- Clark, A., Richardson, R., Ross-Murphy, S., & Stubbs, J. (1983). Structural and mechanical properties of agar/gelatin co-gels: small-deformation studies. *Macromolecules*, 16, 1367–1374.
- Daly, M., & Knorr, D. (1988). Chitosan-alginate complex coacervate capsule: effects of calcium chloride, plasticizers, and polyelectrolytes on mechanical stability. *Biotechnology Progress*, 4, 76–81.
- Denuziere, A., Ferrier, D., & Domard, A. (1996). Chitosan-chondroitin sulfate and chitosan-hyaluronate polyelectrolyte complexes, physico-chemical aspects. *Carbohydrate Polymers*, 29, 317–323.
- Dhami, R., Harding, S., Jones, T., Hughes, T., Mitchell, J., & To, K. (1995). Physico-chemical studies on a commercial food-grade xanthan. Part I. Characterization by sedimentation velocity, sedimentation equilibrium and viscometry. *Carbohydrate Polymers*, 27(2), 93–101.
- Domszy, J., & Roberts, G. (1985). Evaluation of infrared spectroscopic techniques for analysing chitosan. *Makromolekulare Chemie*, 186, 1671–1677.
- Dumitriu, S., & Chornet, E. (1998a). Inclusion and release of proteins from polysaccharide-based polyion complexes. *Advanced drug delivery reviews*, 31, 223–247.
- Dumitriu, S., & Chornet, E. (1998). Polysaccharides as support for enzyme and cell immobilization. In S. Dumitriu (Ed.), *Polysaccharides* (p. 629) Hong Kong: Marcel Dekker, 629.
- Dumitriu, S., & Chornet, E. (2000). *Hydrogels polyioniques à base de xanthane et de chitosane pour la stabilisation et relargage contrôlé, des vitamines*. US Patent No. 09,301,670.
- Dumitriu, S., Chornet, E., & Vidal, P. (1995). *Polyionic insoluble hydrogels comprising xanthan*. WO Patent No. 5,620,706.
- Dumitriu, S., Chornet, E., Vidal, P., & Moresoli, C. (1995b). Polyionic hydrogel as supports for immobilization of lipase. *Biotechnology Techniques*, 9, 836–883.
- Dumitriu, S., Magny, P., Montagne, D., Vidal, P., & Chornet, E. (1994). Polyionic hydrogel obtained by complexation between xanthan and chitosan: their properties as supports for enzyme immobilization. *Journal of Bioactive and Compatible Polymers*, 9(2), 184–210.
- Dumitriu, S., Vidal, P., & Chornet, E. (1998). Hydrogels based on polysaccharides. In S. Dumitriu (Ed.), *Polysaccharides* (p. 125) New York: Marcel Dekker.
- Fukuda, H. (1980). Polyelectrolyte complexes of chitosan and sodium carboxymethylcellulose. *Bulletin of the Chemical Society of Japan*, 53, 837–840.
- Fukuda, H., & Kikuchi, Y. (1978). Polyelectrolyte complexes of chitosan and sodium carboxymethyl dextran. *Bulletin of the Chemical Society of Japan*, 51, 1142–1144.
- Gohel, M., Amin, A., Patel, K., & Panchal, M. (2002). Studies in release behavior of diltiazem HCl from matrix tablets containing (hydroxypropyl) methyl cellulose and xanthan gum. *Bollettino Chimico Farmaceutico*, 141(1), 21–29.
- Ishizawa, C. I. I. (2002). *Chitosan–xanthan hydrogel: a matrix for the inclusion and the delivery of drugs*. PhD thesis, Sherbrooke University.
- Ishizawa, C., Dumitriu, S., & Chornet, E. (2001). *Enhanced solubilization rates of hydrophobic drugs using polyionic chitosan–xanthan hydrogels*. US Patent No. 0,203,962.
- Kikuchi, Y., & Fukuda, H. (1974). Polyelectrolyte complex of sodium dextran sulfate with chitosan. *Makromolekulare Chemie*, 175, 3593–3596.
- Kikuchi, Y., & Noda, A. (1976). Polyelectrolyte complex of heparin with chitosan. *Journal of Applied Polymer Science*, 20, 2561–2563.
- Kobayashi, M. (2001). Structure of gels, characterization techniques. In Y. Osada, & K. Kajiwara (Eds.), *Gels handbook* (p. 172) New York: Academic Press.
- Kondo, T., Irie, T., & Uekama, K. (1996). Combination effects of  $\alpha$ -cyclodextrin and xanthan gum on rectal absorption and metabolism of morphine from hollow-type suppositories in rabbits. *Biological and Pharmaceutical Bulletin*, 19(2), 280–287.
- Kubota, N., & Kikuchi, Y. (1998). Macromolecular complexes of chitosan. In S. Dumitriu (Ed.), *Polysaccharides: structural diversity and functional versatility* (p. 595) New York: Marcel Dekker.
- Lin-Gibson, S., Walls, H. J., Kennedy, S. B., & Welsh, E. R. (2004). Reaction kinetics and gel properties of blocked diisocyanate crosslinked chitosan hydrogels. *Carbohydrate polymers*, 54(2), 193–199.
- Magnin, D., Dumitriu, S., & Chornet, E. (2002). Two applications of a polyionic hydrogel: enzymes immobilization and polypeptides-drug delivery systems. *Advanced materials for biomedical applications. Symposium on advanced materials for biomedical application; COM2002: the conference of metallurgists*.
- Magnin, D., Dumitriu, S., Magny, P., & Chornet, E. (2001). Lipase immobilization into porous chitosan beads: activities in aqueous and

- organic media and lipase localization. *Biotechnology Progress*, 17, 734–738.
- Muzzarelli, R. (1998). Structural and functional versatility of chitins. In S. Dumitriu (Ed.), *Polysaccharides: structural diversity and functional versatility* (p. 569) New York: Marcel Dekker.
- Muzzarelli, R., Rocchetti, R., Stanic, é., & Weckx, M. (1997). Methods for the determination of the degree of acetylation of chitin and chitosan. In R. Muzzarelli, & M. Peter (Eds.), *Chitin handbook* (p. 109) Grottamare: European Chitin Society, Atec Edizioni.
- Park, T. G., Lu, W., & Crotts, G. (1995). Importance of in vitro experimental conditions on proteins release kinetics, stability and polymer degradation in protein encapsulated poly(D,L-lactic acid-co-glycolic acid) microspheres. *Journal of Controlled Release*, 33, 211–222.
- Quemener, B., Marot, C., Mouillet, L., Riz, V. D., & Diris, J. (2000). Quantitative analysis of hydrocolloids in food systems by methanolysis coupled to reverse HPLC. Part 2. Pectins, alginates and xanthan. *Food Hydrocolloids*, 14(1), 19–29.
- Roberts, G., & Domszy, J. (1982). Determination of the viscometric constants for chitosan. *International Journal of Biological Macromolecules*, 4(6), 374–377.
- Ross-Murphy, S. (1991). Incipient behaviour of gelatin gels. *Rheologica Acta*, 30, 401–411.
- Sakiyama, T., Chu, C.-H., & Yano, T. (1993). Preparation of a polyelectrolyte complex gel from chitosan and  $\kappa$ -carrageenan and its pH-sensitive swelling. *Journal of Applied Polymer Science*, 50, 2021–2025.
- Staniforth, J. (2002). Particle-size analysis. In M. Aulton (Ed.), *Pharmaceuticals: the science of dosage form design* (2nd ed.) (p. 152) New York: Churchill Livingstone.
- Stokke, B., Christensen, B., & Smidsrod, O. (1998). Macromolecular properties of xanthan. In S. Dumitriu (Ed.), *Polysaccharides: structural diversity and functional versatility* (p. 433) New York: Marcel Dekker.
- Struszczyk, M. (2002a). Chitin and chitosan. Part I. Properties and production. *Polimeri*, 47, 316–325.
- Struszczyk, M. (2002b). Chitin and chitosan. Part II. Applications of chitosan. *Polimeri*, 47, 396–403.
- Struszczyk, M. (2002c). Chitin and chitosan. Part III. Some aspects of biodegradation and bioactivity. *Polimeri*, 47, 619–629.
- Struszczyk, H., Wawro, A., & Niekraszewicz, A. (1989). Biodegradability of chitosan fibers. In G. Skjak-Braek, T. Anthonsen, & P. Sandford (Eds.), *Chitin and chitosan* (p. 580) London: Elsevier.
- Talukdar, M., den Mooter, G. V., Augustijns, P., Tjandra-Maga, T., Verbeke, N., & Kinget, R. (1998). In vivo evaluation of xanthan gum as a potential excipient for oral controlled-release matrix tablet formulation. *International Journal of Pharmaceutics*, 169(1), 105–115.
- Terbojevich, M., Cosani, A., Foher, B., & Marsano, E. (1993). High-performance gel-permeation chromatography of chitosan samples. *Carbohydrates Research*, 250, 301–314.
- Tschoegl, N. W. (1989). The phenomenological theory of linear viscoelastic behavior: an introduction. Berlin: Springer.
- Tsung, M., & Burgess, D. J. (1997). Preparation and stabilization of heparin/gelatin complex coacervate microcapsules. *Journal of Pharmaceutical Sciences*, 86, 603–607.
- Wang, F., Wang, Y., & Sun, Z. (2002). Food chemistry and toxicology: conformational role of xanthan gum in its interaction with guar gum. *Journal of Food Science*, 67(9), 3289–3295.
- Yamauchi, A. (2001). Gels: introduction. In Y. Osada, & K. Kajiwara (Eds.), *Gels handbook* (p. 4) New York: Academic Press.